340 *Biochemistry* **2011,** *50,* 340–348
DOI: 10.1021/bi101496c

BIOCHEMISTRY
including biophysical chemistry & molecular biology
Article

Light-Induced Conformational Changes in Photosynthetic Reaction Centers: Dielectric Relaxation in the Vicinity of the Dimer[†]

Sasmit S. Deshmukh,[‡] JoAnn C. Williams,[§] James P. Allen,[§] and László Kálmán*[,‡]

[‡]*Department of Physics, Concordia University, Montreal, Quebec H4B 1R6, Canada, and* [§]*Department of Chemistry and Biochemistry, Arizona State University, Tempe, Arizona 85287-1604, United States*

Received September 15, 2010; Revised Manuscript Received December 6, 2010

ABSTRACT: Conformational changes near the bacteriochlorophyll dimer induced by continuous illumination were identified in the wild type and 11 different mutants of reaction centers from *Rhodobacter sphaeroides*. The properties of the bacteriochlorophyll dimer, which has a different hydrogen bonding pattern with the surrounding protein in each mutant, were characterized by steady-state and transient optical spectroscopy. After illumination for 1 min, in the absence of the secondary quinone, the recovery of the charge-separated states was nearly 1 order of magnitude slower in one group of mutants including the wild type than in the mutants carrying the Leu to His mutation at the L131 position. The slower recovery was accompanied by a substantial decrease in the electrochromic absorption changes associated with the Q_y bands of the nearby monomers during the illumination. The other set of mutants containing the Leu L131 to His substitution exhibited slightly altered electrochromic changes that decreased only half as much during the illumination as in the other family of mutants. The correlation between the recovery of the charge-separated states in the light-induced conformation and the electrochromic absorption changes suggests a dielectric relaxation of the protein that stabilizes the charge on the dimer.

The bacterial reaction center (RC)[1] is an intrinsic membrane-bound chromophore−protein complex that serves as the site for the initial photochemical conversion of light excitation energy into chemical free energy (*1*). The RC is composed of three protein subunits termed L, M, and H. The L and M subunits bind the bacteriochlorophyll, bacteriopheophytin, and quinone cofactors that are arranged pseudosymmetrically with respect to the axis connecting the bacteriochlorophyll dimer, P, and the ferrous ion (*2*, *3*). Light initiates the transfer of an electron from P via intermediate acceptors, involving a bacteriochlorophyll monomer (B) and bacteriopheophytin (H), to the primary quinone (Q_A), followed by transfer to the secondary quinone (Q_B).

The solvation of the newly created charges by individual electron transfer steps is often facilitated by secondary, compensating charge motions, which are coupled to conformational movements in the RC chromophore−protein complex. Because the absorption bands of the individual chromophores are sensitive to changes in their nearby protein environment, both optical and Stark spectroscopies are useful tools for probing the changes of the local electrostatic properties upon excitation and relaxation. Stark spectroscopy had been applied successfully to monitor these changes not only in RCs of purple bacteria but also in the photoactive yellow protein, where large photoinduced conformational changes were identified by detecting the band shifts of the chromophores (*4*, *5*). Stark spectroscopy requires the use of cryogenic temperatures to keep the studied molecules oriented with respect to the externally applied electric field and, thus, cannot be used to follow the conformational changes in real time. Moreover, the cooling of the samples to cryogenic temperatures induces structural changes, for example, as evidenced by the shift of the Q_y absorption band of P from 865 nm measured at room temperature to 890 nm at 77 K (*6*). Further complications can be introduced with the addition of glycerol as a cryoprotectant as it increases the viscosity of the samples and thus can alter the kinetics of the conformational changes. The internal electric field generated by charge separation is always oriented in each RC, and the electrochromic absorption changes are quite pronounced in the light-minus-dark optical difference spectrum even at room temperature. To investigate the changes in the local electric field due to the conformational changes, the band shifts of the tetrapyrrols at physiologically relevant temperatures were monitored using optical spectroscopy.

Descriptions of a functioning RC call attention to the important role of protein motion and conformational reorganization in the electron transfer process over a wide range of time scales from nanoseconds to minutes (*7*−*19*). Proposals for conformational changes occurring on the second to minute scales at room temperature stem primarily from the observation of multiphasic kinetics in the light-induced optical absorption changes (*15*−*18*, *20*). Much of this spectroscopic work has centered on the quinones primarily because direct evidence of structural changes in the Q_B region and in the H subunit was obtained by determining the structure of the RC in the light-activated state by X-ray crystallography (*21*, *22*). In contrast to the detailed information concerning the conformational changes near the quinones, no specific light-induced structural changes involving the tetrapyrroles or specific amino acid residues near the periplasmic side have been identified.

[†]This work was supported by grants from the Natural Sciences and Engineering Research Council of Canada (to L.K.) and the National Science Foundation (MCB 0640002 to J.P.A.).

*To whom correspondence should be addressed. Phone: (514) 848-2424, ext. 5051. Fax: (514) 848-2828. E-mail: laszlo.kalman@concordia.ca.

[1]Abbreviations: RC, reaction center; P, bacteriochlorophyll dimer; B, bacteriochlorophyll monomer; H, bacteriopheophytin; Q_A, primary quinone; Q_B, secondary quinone; WT, wild type; H-bond, hydrogen bond; LDAO, lauryl dimethyl amine oxide.

 Published on Web 12/08/2010

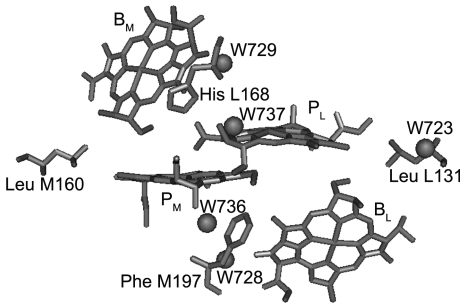

FIGURE 1: Structural view of the four bacteriochlorophylls constituting the dimer (P_L and P_M) and the monomers (B_L and B_M) with the nearby amino acid residues and internal water molecules. The four residues, Leu L131, Leu M160, His L168, and Phe M197, were modified to introduce or remove H-bonds. Five water molecules, W723, W728, W729, W736, and W737 (spheres), were identified in the immediate vicinity of the bacteriochlorophylls. Coordinates were taken from Protein Data Bank entry 1PCR (*44*).

A number of specific interactions of amino acid residues with P have been investigated. The two halves of P contain two π-conjugated groups: the 2-acetyl and the 9-keto carbonyl that are possible proton acceptors for hydrogen bonds (H-bonds). Structural and spectroscopic data demonstrated that in the wild-type (WT) *Rhodobacter sphaeroides* RC only one H-bond exists between His L168 and the 2-acetyl group of the L half of the dimer (P_L) in addition to the Mg-coordinating His residues at L173 and M202 (*2*, *23*, *24*). A series of mutants have been constructed to modify the H-bonding pattern on the conjugated carbonyl groups of P by introducing histidine residues into each H-bonding position or replacing His L168 (Figure 1) (*25*). In the mutants, Leu to His at L131, Leu to His at M160, Phe to His at M197, and His to Phe at L168, the formation and removal of H-bonds were confirmed by Raman, infrared, and special triple spectroscopies (*26*−*28*). Even though the spectroscopic properties of these mutants, including the shifts of the Q_y band of P caused by the mutations, have been extensively studied in the past, the shifts of the absorption bands of the surrounding cofactors upon illumination have not yet been scrutinized (*6*, *29*). For shorter abbreviations, the mutants will be identified in the text by only the position of the mutation.

In this paper, we report the effects of alterations in amino acid side chains near P on the light-induced conformation of RCs, as evidenced by the correlation between the electrochromic absorption changes of the light-minus-dark difference optical spectra and kinetics of the charge recombination after prolonged illumination.

EXPERIMENTAL PROCEDURES

Mutagenesis, Bacterial Growth, and RC Isolation. The construction of the mutant strains of *Rba. sphaeroides* by oligonucleotide-directed mutagenesis has been described previously (*29*−*31*). The genes were expressed in *Rba. sphaeroides* deletion strain ΔLM1.1 (*32*). The term WT used in this paper refers to the deletion strain complemented with a plasmid bearing the WT RC genes. The strains were grown under nonphotosynthetic conditions, and the RCs were isolated using procedures described previously (*30*). RCs were kept in 15 mM Tris-HCl (pH 8.0), 0.1% lauryl dimethyl amine oxide (LDAO), and 1 mM EDTA. The purity of the RCs, defined as the ratio of the absorbance at 280 nm to that at 802 nm, was between 1.2 and 1.5 for all preparations.

Optical Spectroscopy. The light-minus-dark optical difference spectra and the kinetics of the absorbance changes were determined using Varian (Mulgrave, Victoria, Australia) Cary 5 and 5000 spectrophotometers with scanning rates of ~900 and ~1800 nm/min. The samples were prepared under very weak green light and were adapted to the dark in the spectrometers for ~30 min before being exposed to any illumination. The light-induced states of the RCs were generated by continuous illumination through an 870 ± 20 or 850 ± 20 nm interference filter using a halogen lamp. The light intensity was set to ~30% of the saturating value for WT at an RC concentration of 2 μM. The kinetic traces were analyzed by decomposing them into exponentials using a Marquardt algorithm. Terbutryne was used at a concentration of 100 μM to eliminate secondary quinone activity. All measurements were performed at room temperature.

RESULTS

Light-Minus-Dark Difference Optical Spectra. In the presence of terbutryne, the light-induced changes in the optical spectra of WT and the 11 mutants exhibited characteristic features associated with both P^+ and Q_A^-. These changes include an absorption decrease of the Q_y band of P centered at 865 nm in WT but varied in the mutants, an electrochromic blue shift on the B region around 800 nm and an electrochromic red shift on the H-band around 760 nm. Figure 2 shows these absorption changes recorded 1 min after the illumination had begun. The observed variations in the light-minus-dark spectra of the mutants involved differences in the position of the Q_y band of P, and in the extent of the electrochromic changes around the B bands (vertical lines in Figure 2). Some characteristic differences were also found in the spectra of the individual mutants recorded at different times during and after the illumination as discussed later. The position of the Q_y band of the dimer showed some correlation with the introduced H-bonds. Generally, the formation of an H-bond with P_M resulted in a blue shift in the position of the P-band, and the introduction of the H-bonds with P_L caused red shifts in this parameter. Table 1 and Figure S1a of the Supporting Information summarize the observed peak positions of the P band after 1 min illumination upon addition of each H-bond at the L168, M197, L131, and M160 positions. For example, the presence of the H-bond between the 2-acetyl group of the P_L and the His L168 in the WT RC resulted in a 16 nm red shift relative to the position of the P band in the L168 mutant, which lacks any of the H-bonds. Interestingly, comparison of mutants with the symmetrical H-bond between the 2-acetyl group of P_M with the His substitution at the M197 position shows almost the same value of 17 nm upon comparison of mutants with and without the His L168 change, namely, the M197 and M197+L168 double mutant. Formation of H-bonds with the 9-keto groups on both sides of P showed smaller quasi-symmetrical shifts of 9 nm to the blue and 7 nm to the red in the M160+L168 and L168+L131 double mutants, respectively, compared to the L168 mutant. The differences in the position of the P band were smaller in mutants with more than one H-bond. For example, the hypsochromic shifts resulting from the H-bond at P_M in the M160 and M197 mutants are only 1−3 nm relative to the WT, which has one H-bond. A bit larger bathochromic shift of 5 nm was observed in the presence of the H-bond at P_L in the L131 mutant. With the increase in the number of H-bonds from two to three and from three to four, the observed shifts of the dimer band from 865 nm became negligible (Figure 1 and Figure S1a of the Supporting Information).

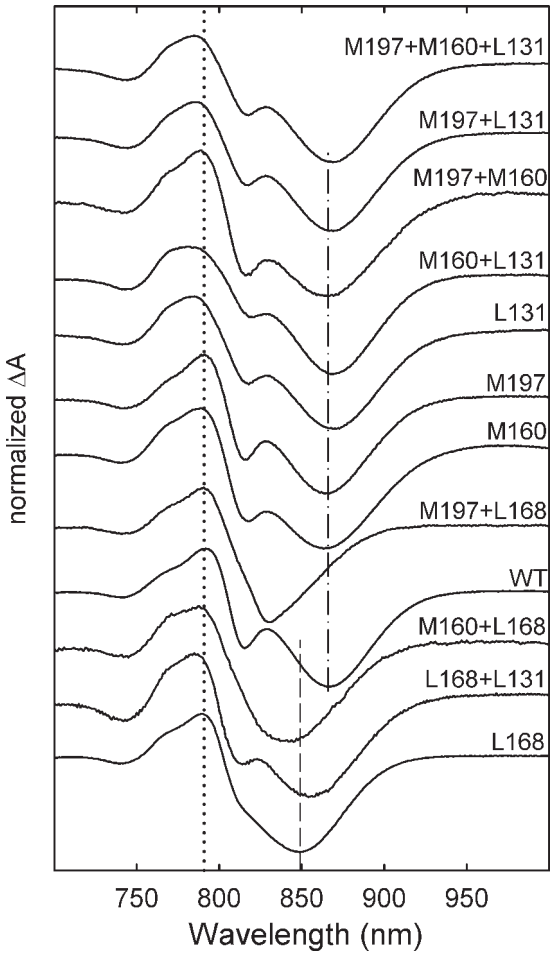

FIGURE 2: Near-infrared light-minus-dark optical difference spectra of RCs isolated from WT and 11 hydrogen bonding mutants. The spectra were recorded after continuous illumination for 1 min and were normalized to the center of the Q_y band of the dimer (832−870 nm depending on the mutant). The position of the dimer (—·—), the position of the positive band of the electrochromic absorption change of the monomers in the WT (···), and the position of the dimer in the L168 mutant (− − −) are indicated by vertical lines for reference. The spectra are approximately arranged in increasing order of oxidation potential of the dimer (from ref *25*). Conditions were as follows: 2 μM RC in 15 mM Tris (pH 8), 0.1% lauryl dimethyl amine oxide, 1 mM EDTA, 100 mM NaCl, and 100 μM terbutryne. The illumination time was 1 min (through a 870 nm interference filter using a water bath as a heat filter). The scanning rate was 800 nm/min.

Differences were also found in the electrochromic absorption changes involving the bands of B_L and B_M near 800 nm. The basis of the comparison was the position of the positive peak centered at 790 nm in the WT spectrum (Figure 2, vertical dotted line). The RCs that have H-bonds at the L131 position exhibited a 6−9 nm blue shift in the position of this peak relative to the WT, while the other mutations resulted in only 0−2 nm changes. This trend is clearly visible in Figure S1b of the Supporting Information, where the change in the position of the positive band near 790 nm is plotted as a function of the number of H-bonds upon introduction of any new H-bond into a particular mutant.

Kinetics of Formation and Recovery of Light-Induced States. The kinetics of the absorption changes caused by non-saturating illumination were measured at the center of the Q_y band of the dimer observed in the RCs from each mutant (Figure 3). In the presence of terbutryne, the $P^+Q_A^-$ state was formed immediately after the light was turned on, resulting in a rapid absorption change. In addition, a further slower bleaching was also observed in all RCs. Because the excitation was sub-saturating, with only ~30% of WT RCs excited at the beginning of the illumination, this slow increase can be interpreted as arising from another light-induced state being formed with a longer lifetime. Once the light is turned off, complex recovery kinetics that depended on the duration of the illumination and the mutation are observed (Table 1). For most measurements, the RCs were poised at pH 8.0 and illuminated for 1 min for comparison of the recovery kinetics of the oxidized dimer in the mutants after prolonged illumination. During this 1 min illumination, the optical absorbance changes reached their saturating values in all mutants and were fully reversible even in the mutants with high dimer potentials. After the illumination was turned off, a fraction of the RCs followed the fast $P^+Q_A^- \rightarrow PQ_A$ charge recombination while the rest of P^+ recovered on a much longer time scale. In RCs containing the Leu to His mutation at the L131 position, the slower component of the P^+ decay had a lifetime of 7−8 s, corresponding to rate constants of $1.2-1.4 \times 10^{-1}$ s^{-1}. Contrarily, in RCs without this mutation, this kinetic parameter was much longer, with lifetimes of 30−63 s, corresponding to rate constants of $1.6-3.3 \times 10^{-2}$ s^{-1}. The L168+L131 and M160+M197 mutants exhibited intermediate values with 11 and 14 s lifetimes, or k_{slow} values of 9.58×10^{-2} and 7.1×10^{-2} s^{-1}, for that slow phase, respectively. It should be mentioned that after illumination for only a few seconds the kinetic traces of both sets of mutants were similar and the components with rate constants of ~10^{-2} s^{-1} could not be detected in the WT family; instead, the components with rate constants of ~10^{-1} s^{-1} were seen just like in the mutants with the H-bond at the L131 position (data not shown). The relative amplitude of the slow phase in the formation (during the illumination) and recovery (in dark) was much smaller in the case of the L131 family of mutants and the M160+M197 double mutant compared to the rest of the mutants (Figure 3).

Correlation between the Slow Kinetic Components and the Light-Induced Spectra. Comparison of the results shown

Table 1: Kinetic and Steady-State Optical Spectroscopic Parameters of the WT and 11 H-Bond Mutants Measured in RCs of *Rba. sphaeroides*

mutant[a]	P position[b] (nm)	position 790[c] (nm)	k_{slow} decay[d] ($\times 10^2$ s^{-1})	no. of H-bonds[e]
L168	849	790	1.63	0
M160+L168	840	788	1.72	1
M197+L168	832	790	1.69	1
WT	865	790	1.96	1
M160	862	788	2.56	2
M197	863	790	3.33	2
M197+M160	864	788	7.14	3
L168+L131	856	784	9.58	1
L131	870	784	14.28	2
M160+L131	868	781	12.50	3
M197+L131	865	782	12.51	3
M197+M160+L131	865	784	14.28	4

[a]Only the positions where the mutations were made are shown. The exact substitutions are listed in the beginning of the paper. [b]Position of the Q_y band of the dimer in the light-minus-dark difference spectra of the mutants in Q_A active RCs (data taken from Figure 2). [c]Position of the lower-wavelength band of the electrochromic shift on bacteriochlorophyll observed at 790 nm in the light-minus-dark difference spectrum of the WT (data determined from Figure 2). [d]Rate constants of the slowly decaying component of P^+ after illumination for 1 min (determined from Figure 3). [e]Number of H-bonds to P in the mutants.

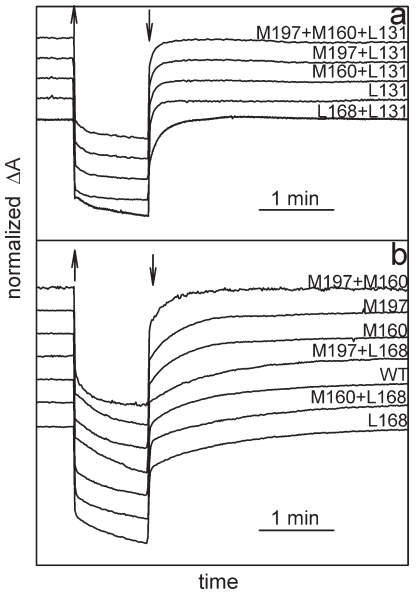

FIGURE 3: Formation and disappearance of the continuous light-induced $P^+Q_A^-$ redox states in the WT and 11 hydrogen bond mutants measured at the position of the P band (832−870 nm depending on the mutant) at pH 8. (a) Mutants containing the Leu to His mutation at the L131 position. (b) All other mutants and WT. The illumination time is 1 min. The traces were normalized and vertically shifted for better comparison. The vertical up and down arrows indicate when the illumination was turned on and off, respectively. Conditions as described in the legend of Figure 2.

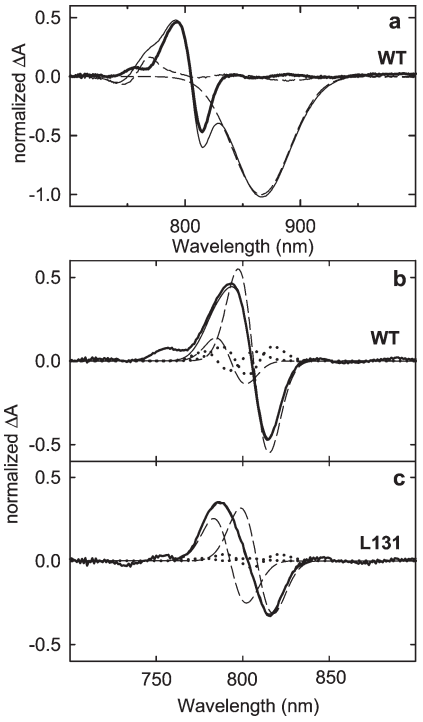

FIGURE 4: Analysis of the near-infrared light-minus-dark difference optical spectra. Panel a shows the treatment for the WT RC. The contribution of the dimer band and the Q_A^-/Q_A difference spectrum (− − −) were subtracted from the spectrum measured after illumination for 1 min (thin solid line). The resulting trace (thick solid line) represents the electrochromic absorption changes of B_L and B_M. Panels b and c show the electrochromic absorption changes of B_L and B_M after the subtractions performed in the spectra of WT and the L131 mutant, respectively. The electrochromic absorption changes were analyzed in terms of shifts (− − −) and broadenings (· · ·) of the Q_y absorption bands of B_L and B_M. The conditions and the parameters of the fit are described in the text and listed for all mutants in Table S1 of the Supporting Information.

in Figures 2 and 3 and also Figure S1a,b of the Supporting Information suggests that there is no obvious correlation between the position of the Q_y band of P and the kinetics of the recovery of the charge pair after continuous illumination. Because the RCs contain only Q_A and not Q_B due to the addition of the terbutryne, no significant differences are expected among the mutants in the spectra or kinetics due to Q_A^-. On the other hand, the 6−9 nm blue shift from 790 nm in the light-minus-dark spectra (Figure 2 and Figure S1b of the Supporting Information) in the mutants carrying the Leu to His mutation at the L131 position was coupled to faster recovery kinetics of the $P^+Q_A^-$ charge pair after the continuous illumination was turned off. On the basis of this correlation, we decided to investigate the electrochromic absorption changes in the accessory B region around 800 nm thoroughly. These spectral changes are sensitive to the alteration of the local electric field near the B molecules because of both the charge separation and the conformational changes proposed in this work. Even though the resolution and the assignments of the spectral features would be more accurate in low-temperature spectra, we decided to perform the analysis at room temperature. Cooling the samples to cryogenic temperatures introduces additional changes in the spectra as mentioned earlier, and it would be difficult to separate these changes from those that were caused exclusively by the prolonged illumination. In the room-temperature, light-minus-dark spectra presented in Figure 2, the electrochromic changes near 800 nm are partially overlapped with contributions associated with the formation of Q_A^- and bleaching of the P band. These overlapping contributions were removed by subtraction of the light-induced Q_A^-/Q_A difference spectrum and the photobleached P band from the light-minus-dark difference spectrum for each mutant and the WT. The resulting spectra contain spectral signatures that are exclusively characteristic of the accessory B monomers. The light-induced Q_A^-/Q_A difference spectra were recorded in each mutant and the wild type in the presence of a secondary electron donor, ferrocene (data shown for only the WT). The dimer band was fitted with a Gaussian curve in each mutant using the absolute near-infrared spectra (data not shown). The treatment of the light-minus-dark difference spectra is presented for the WT as an example in Figure 4a. In the analysis, each monomer B is modeled as giving rise to an absorption band near 800 nm (794 and 810 nm for B_A and B_B, respectively) with three parameters, namely amplitude, width at half-maximum, and position. The spectra were fitted assuming that the 800 nm band is due to the two B monomers with each absorption band shifting and broadening in response to illumination. The resulting spectra featuring only the electrochromic absorption changes of the B monomers are shown for two representative RCs: the WT and the L131 mutant in panels b and c of Figure 4, respectively. For the entire set of studied RCs, these spectra can be reviewed in Figure S2 of the Supporting Information. The light-induced electrochromic absorption changes of the accessory B monomers were analyzed by assuming shifts and broadenings of the bands of B (B_L and B_M) upon illumination for 1 min. The parameters of the fits for all mutants and the wild type are listed in Table S1 of the Supporting Information. Shifts in the absorption band of a chromophore are generally due to the change in the polarizability, while band broadenings are associated with the change in the dipole moment of the chromophore (*33*). The positions and the widths

at half-maximum of the bacteriochlorophyll monomer bands were determined by Gaussian fits from the absolute absorption spectra of each RC, assuming equal bands for each of the B monomers (data not shown) as introduced previously (*34*). The observed position of the B band at 803 nm is remarkably conserved in the room-temperature absolute optical spectra of the mutants in this study and even in mutants that contain five or six amino acid substitutions near the dimer (*35*). The contributions of the two B monomers, however, to the light-induced spectra were found to be significantly different in the two groups of mutants. In the mutants containing the Leu to His mutation at the L131 position, the hypsochromic shift of the B_M band from 810 nm was only 4.1−5.3 nm, while in the rest of the mutants including the WT, this shift was approximately twice as large (6.9−11.3 nm). Contrarily, the blue shift of the B_L band from 794 nm was found to be slightly larger in the group of the L131 family with values of 2.5−3.8 nm compared to the 0.3−2.7 nm shift in the family that lacks this mutation. It should be noted that the mutants that have no H-bonds with P_L at all (L168, L168+M160, and L168+M197) exhibited negligible shifts in the B_L band and the largest shifts in the B_M band with values of 0.3−2.0 and 9.6−11.3 nm, respectively. In summary, the light-induced electrochromic shifts were almost balanced between the bands associated with B_L and B_M in the L131 family, whereas in the group whose members lack this mutation, the shift of the B_M band outweighed the small to negligible shift of the B_L band. Small broadenings with decreased peak absorbances had to be considered in most cases, indicating that not only the polarizability but also the dipole moment of the B molecules is changing upon illumination. These broadenings, however, were much less prominent than the shifts and mostly were below 1 nm (Figure S2 and Table S1 of the Supporting Information).

Illumination Time Dependence of the Light-Induced Spectral Changes. Near-infrared light-induced spectra were recorded at different times during and after the illumination for the studied RCs with a 1800 nm/min scanning rate. Figure 5a shows traces for WT and for the L131 mutant representing the two groups of RCs. For each sample, four spectra were measured: immediately after the onset of the illumination, after illumination for 1 min, 1 min after the illumination ceased, and 6 min after the illumination ceased (labeled A−D, respectively, in Figure 5a). The spectra were normalized to the bleaching of the P band because it had been demonstrated previously using a very high (1 W/cm^2), saturating illumination intensity that the oscillator strength of this band does not change during the illumination (*16*). It is clearly visible in the spectra that the absorption changes associated with the B monomers around 800 nm are the largest immediately after the onset of illumination both in the WT and in the L131 mutant (traces A in Figure 5a). With increasing illumination time, these changes decreased with respect to the extent of P^+. After illumination for 1 min, the decreases in the electrochromic absorption changes of the B bands were approximately twice as large in the WT versus the L131 mutant as evidenced by the double difference spectra (traces A and B in Figure 5a, and the difference spectrum, namely trace B minus trace A in Figure 5b). Similar trends were observed for the other members of the two groups of mutants (data not shown). In Figure 5a, we also show the spectra recorded 1 min after the illumination was turned off (traces C). For the WT, this spectrum represents the population of the RCs still in the $P^+Q_A^-$ state but exclusively in the light-adapted conformation, while for the L131 mutant, the spectrum reflects the light-adapted PQ_A ground state (see the

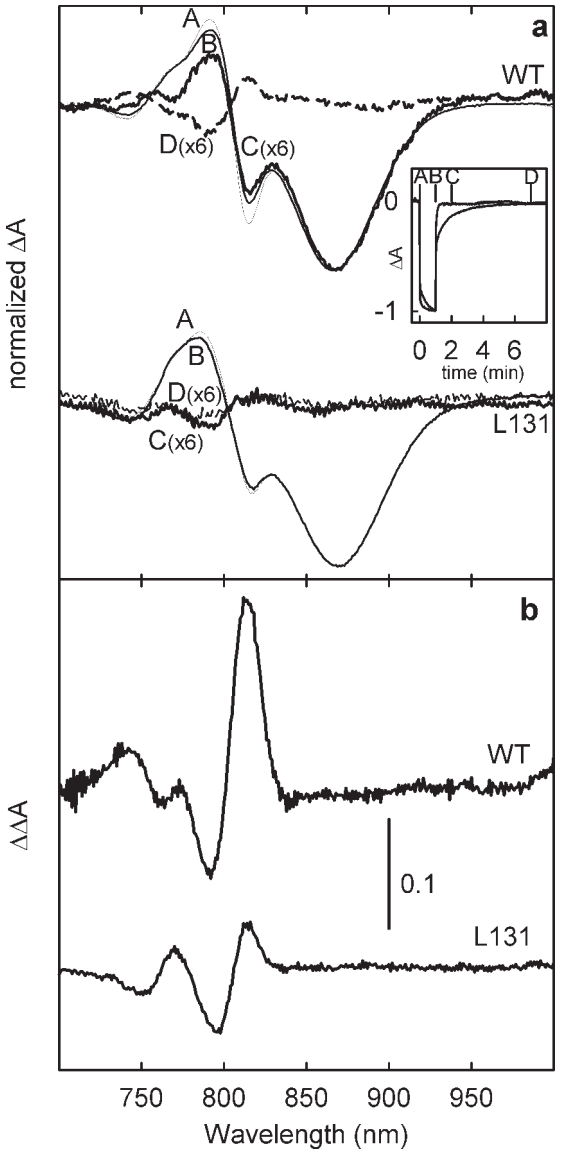

FIGURE 5: (a) Normalized light-minus-dark optical difference spectra of WT and the L131 mutant recorded immediately after the light had been turned on (traces A), after illumination for 1 min (traces B), and 1 and 6 min after the illumination had been turned off (traces C and D, respectively). Traces C and D were magnified by 6-fold to match the absorption change at 865 nm with traces A and B in WT and also to emphasize the residual absorption changes around 800 nm. The inset shows the time dependence of the absorption changes and indicates the times at which the spectral traces were recorded. (b) Double difference spectra (traces B minus A from panel a) for the WT and for the L131 mutant. Conditions as in Figure 2 except the traces were recorded at a scanning rate of 1800 nm/min.

inset in Figure 5a). It should be noted that spectra recorded 6 min after the light was turned off still contained absorption changes around 800 nm in all samples even after the $P^+Q_A^-$ charge pair recovered completely (traces D of Figure 5a). All of these spectra recovered to the ground state ~1 h after it had been exposed to illumination for 1 min. With the use of longer illumination times (5−15 min), these residual signals were visible even after several hours (data not shown). Similar long-lasting absorption changes around 800 nm were observed but not discussed earlier both in the low-temperature spectra and in the room-temperature spectra for RCs dispersed either in LDAO or in *n*-dodecyl *β*-D-maltoside after prolonged continuous illumination or trains of flashes (*17*, *18*, *39*). Analysis of the spectra for WT (traces A and C of Figure 5a) as

described above and shown in Figure 4 confirmed that the B_B band that has been blue-shifted from 810 to 801 nm as a result of the onset of the illumination moved back to 804 nm during the 1 min illumination in those fractions of the RCs that exhibited long recovery kinetics of the $P^+Q_A^-$ charge pair. No such relaxation of the B_A band could be observed. Because of the much shorter lifetime of the $P^+Q_A^-$ state in the L131 mutant, only the spectra recorded under illumination could be analyzed with the same emphasis (traces A and B). Only ~1 nm differences in the positions of the B_L and B_M bands could be determined as the illumination time increased from 0 to 1 min with values of 790−791 and 805−806 nm, respectively. From the illumination time dependence of the electrochromic absorption changes, we conclude that prolonged illumination causes dielectric relaxations in the RCs near P^+ resulting in the smaller electrochromic absorption changes in the nearby B bands. In the WT, this relaxation was approximately twice as large as that found for the L131 mutant and predominantly involved B_B, whereas in the L131 mutant, they affected both monomers. The absorption changes around 800 nm remained detectable for up to 1 h in the spectra under the conditions used. It must also be noted that in the spectra recorded 1 min after the illumination had been turned off the electrochromic absorption changes near 760 nm have also decreased in all of the mutants of the WT family, where the long-lived charge-separated states could still be detected. This is indicative of a similar dielectric relaxation near the H molecules, most likely due to the stabilization of Q_A^- and/or the weakening of the long-range electrostatic interactions between P and H molecules due to the structural changes near P.

DISCUSSION

RCs from WT and 11 mutants with different combinations of H-bonds involving the 2-acetyl and 9-keto carbonyl groups of P and the surrounding protein environment have been exposed to continuous illumination (Figure 1). The effect of prolonged illumination near P was studied by comparing the light-minus-dark difference optical spectra and the kinetics of the recovery of the light-induced states. Because the genetic modifications involved only the immediate vicinity of P, all RCs contained the same intact quinone binding pockets. A crystal structure reported for a mutant that was designed to bind and oxidize metal ions and contains all four possible H-bonds at the L168, L131, M197, and M160 positions exhibited no significant structural changes near P except the amino acid substitutions in comparison with the structure of the WT (*35*). In this work, a strong correlation was found between the magnitudes of the electrochromic absorption changes of the light-minus-dark difference optical spectra involving the B bands (Figures 2 and 4) and the lifetime of the long-lived charge-separated state (Figure 3). The RCs that initially exhibited large electrochromic shifts in the B_M band but decreased shifts upon illumination have shown significantly longer lifetimes for the long-lived $P^+Q_A^-$ charge pair. This connection between the dielectric relaxation near P and the light-induced conformational changes is discussed.

Electron Transfer Rates in Different Conformational States. All 12 studied RCs exhibited complex recovery kinetics for the $P^+Q_A^-$ charge pair after illumination for 1 min with rate constants for the slow kinetic component ranging from 1.63×10^{-2} to 1.42×10^{-1} s^{-1} (Figure 3). The flash-induced $P^+Q_A^- \rightarrow PQ_A$ charge recombination is expected to be a single-exponential decay in the WT and the mutants used in this work with rate constants ranging between 4.5 and 25 s^{-1} (*36*). Even if the Q_B activity of the RCs is retained, there must be two components in the charge recombination kinetics in WT RCs with rate constants of ~10 and ~1 s^{-1} at pH 8 (*37*). It has been shown previously by several groups that continuous illumination generates a heterogeneous population of detergent-isolated RCs that have significantly longer lifetimes for the $P^+Q_A^-$ or $P^+Q_B^-$ charge pairs in the WT and in the R-26 strain compared to those obtained after single-flash excitation (*15*−*18*, *20*, *38*, *39*). The longer lifetimes determined using prolonged illumination were attributed to the recombination of the charge pairs in RCs that adopt different conformations induced by the illumination. The quantum yields of the proposed conformational changes were found to be low, and the light-adapted conformations could not be detected in the kinetic traces using single-flash excitation. During continuous illumination or trains of flashes, however, these altered conformations can be built up because of the long lifetimes of the charge-separated states in these different conformers. Although earlier studies used various different conditions (temperature, pH, detergent environment, illumination time and intensity, Q_B occupancy, etc.) that influence the recovery kinetics, the lifetimes determined in this study for the WT are in good agreement with those previously reported for the WT and R-26 (*16*, *18*, *20*). The lifetime and the number of the kinetic components are variable and dependent on the illumination time, indicating that the conformational changes are strongly linked and some involve consecutive reactions (*16*, *20*). After the sample had reached equilibrium, two major components can be distinguished at pH 8 that are characteristic of the dark-adapted and one kind of light-adapted conformation, depending upon the conditions, such as pH and detergent environment as described elsewhere (*16*). The individual conformational changes that give rise to different lifetimes have not been identified yet at the molecular level, although most of the studies so far proposed conformational changes near the quinones (*15*, *17*, *18*, *39*), as supported by X-ray crystallographic analysis of the RCs that had been illuminated (*21*, *22*, *40*). These studies, however, were either conducted at cryogenic temperatures or used very short, subsecond illuminations because it was found that the detergent-grown crystals do not diffract when exposed to prolonged illumination (*40*). The formation of the long-lived charge-separated states investigated in this work and many previous kinetic studies certainly requires an illumination time of much longer than 1 s at room temperature (Figure 3) (*15*−*18*, *20*). Crystallographic and FTIR spectroscopic studies provided opposing models with regard to the movement of Q_B itself (*21*, *41*, *42*). Thus, while there is no doubt regarding the conformational changes near the cytoplasmic site of the RC, it is questionable whether the low-temperature, light-induced X-ray crystallographic studies are fully applicable to the conformational changes observed at room temperature during illuminations that are orders of magnitude longer than subseconds. In this study, we attempt to localize the conformational changes that give rise to the longest-lived kinetic component in the recovery kinetics after illumination for 1 min. In Figure 6, we plotted the relative rate constants of the slowest kinetic component found in each mutant with respect to those measured for the WT ($k_{slow}^{mutant}/k_{slow}^{WT}$) as a function of the number of H-bonds. We grouped the mutants on the basis of the location of the H-bonds found in the L131, L168, M160, and M197 positions. The rate constants of the slowest kinetic component that represent the recovery of the $P^+Q_A^-$ state in the one kind of light-adapted conformation in four mutants with the H-bond of

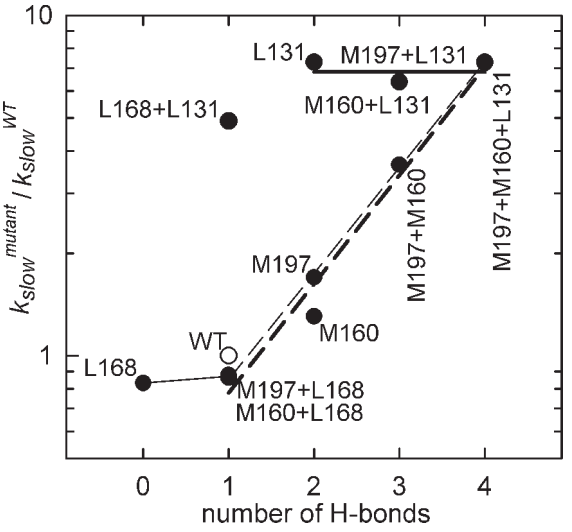

FIGURE 6: Dependence of the relative rate constant ($k_{slow}^{mutant}/k_{slow}^{WT}$) of slow recovery of the oxidized dimer on the number of H-bonds. The mutants are numbered according to Table 1. Regression lines were generated through the data points associated with the mutants having H-bonds created with the dimer at positions L131 (thick solid line), M160 (thick dashed line), and M197 (thin dashed line) or the existing H-bond removed at L168 (thin solid line). The rate constants were determined from Figure 3 and were taken from Table 1.

P_L at the L131 position (L131, M160+L131, M197+L131, and M160+M197+L131) showed no dependence on the number of H-bonds and were ~7 times higher than that measured in the WT. Similarly, the rate constants in the mutants that lack any H-bond with P_L (L168, L168+M160, and L168+M197) exhibited quasi independence from the number of H-bonds, while they were even slightly smaller than that in the WT. The L168+L131 double mutant that lacks the H-bond at the L168 position but has the one at the L131 position has been excluded from both groups, although it showed more similarity to members of the L131 family of mutants (Figure 6). It appears that the presence of the H-bond between P_L and the L131 His is not allowing the formation of the longest-lived charge-separated state regardless of whether the H-bond at the M160 or M197 position is established with P_M if a 1 min illumination is used. On the other hand, the lack of any H-bond with P_L favors formation of the long-lived charge-separated state despite the presence of the H-bonds with P_M. Furthermore, the rate constants in the mutants having H-bonds introduced into P_M either at the M160 or at the M197 position exhibited a very pronounced and similar dependence on the number of H-bonds, provided the H-bond at L168 with P_L was established (Figure 6). It is not obvious whether the H-bonds at the M160 and M197 positions have the same influence because two of the mutants (M197+M160 and M197+M160+L131) have both H-bonds. More evidence points toward the importance of the M197 position as the orientation of the 2-acetyl group of P_M can be different when free or H-bonded (*28*). Nonetheless, the lifetime of the long-lived charge-separated state is clearly sensitive to the number of H-bonds with P_M, provided the H-bond with P_L at the L168 position is present, but it becomes independent of it if either the H-bond with P_L at L131 is present or that at L168 is removed.

Alterations in the Local Electric Field by the H-Bonds. The addition of the H-bonds may alter the local electric field by at least three mechanisms: (i) modifying the local dielectric constant by substituting more hydrophilic residues, (ii) changing the spin density distribution between the two halves of P, and (iii) displacing structural water molecules. The H-bonds were created by substituting His residues for the highly hydrophobic residues, such as Leu or Phe, or the existing H-bond was removed by substituting the His with a highly hydrophobic Phe residue. These substitutions in the immediate vicinity of the dimer should modify the local dielectric constant and therefore the electrochromic absorption changes of the nearby B_L and B_M molecules. In the mutants that contained the H-bond between the P_L and the L131 His residue, the contribution of the B_M band to the electrochromic absorption changes was only approximately half of what was found for the other family of mutants including WT (Figure 4 and Figure S2 and Table S1 of the Supporting Information). The smaller contribution of the B_M band even without a detailed analysis can be observed as the shift of the positive absorption peak near 790 nm by 6−9 nm toward the blue spectral range of the light-minus-dark difference spectra in the mutants with the Leu to His substitution at the L131 position (Figure 2 and Figure S1b of the Supporting Information). In the rest of the mutants and the WT, this shift was only 0−2 nm. It has been suggested that the local dielectric constant in the active, L branch near P is significantly larger than in the inactive, M branch (*4*). Because the interaction energies causing the electrochromic absorption changes are inversely proportional to the dielectric constant, the large difference in the electrochromic shifts of the B_M and B_L bands reported here for WT is in agreement with the assumption of a lower dielectric constant in the M branch (Figure 5). Substitution of a hydrophilic His residue near P increases not only the local dielectric constant but also the alteration of the sharing of the unpaired electron between the two halves of P upon formation of P^+. Special Triple ENDOR spectroscopy showed that in WT the unpaired electron is residing on P_L and P_M with an ~2:1 ratio favoring P_L, whereas in the L131 mutant, it is distributed almost equally between the two halves of P (*28*). This trend is visible for all mutants that contain the Leu to His substitution at the L131 position. The addition of the H-bond at the L131 position in all mutants lowered the spin density ratio on P_L by ~0.1−0.3, and with any given number of H-bonds, the mutants that possess the H-bond at the L131 position have the smallest spin densities on P_L compared to those that lack the Leu to His substitution at the L131 position (Figure S1c of the Supporting Information). The increase in the spin density on P_M at the expense of that on P_L in the L131 mutant should decrease the magnitude of the electrochromic absorption changes of B_M because the axis of the Q_y transition (along the A and C rings) of B_M is closer to the plane of P_L than P_M (Figure 1). Moreover, B_M is ~2 Å closer to P_L than to P_M (*43*). This is in agreement with the observed decrease in the contribution of B_M to the electrochromic absorption changes in the L131 mutant compared to the WT (Figure 4b,c). The variation in spin density, however, does not fully account for the observed trend in the electrochromic absorption changes and the kinetics in the 11 mutants, not to mention the dielectric relaxation during the illumination shown in Figure 5. For example, both in the M160+L168 and in the M160+L131 mutants, the spin density distribution is very similar to that in the WT (~2:1 favoring P_L), but the kinetics of the absorption changes were ~7 times faster in the M160+L131 mutant than in the M160+L168 mutant and WT (Figure 3 and Table 1). Similarly, the electrochromic absorption changes were found to be quite different in these three RCs (Figure S2 of the Supporting Information).

Internal Water Molecules. The X-ray crystal structure of the WT RC identified five water molecules near the immediate

vicinity of the four bacteriochlorophylls (*43*) (Figure 1). All five water molecules are in key positions in terms of their potential to influence the electrochromic absorption changes. Two of the water molecules, namely, W728 and W729, appear to play clear structural roles as they bridge the B monomers, being within H-bond distance of the 9-keto carbonyl groups of B_L and B_M with distances of 2.7 and 2.8 Å, respectively, and also H-bonded to His M202 and L173 that coordinate the central Mg^{2+} of P_M and P_L. In these bridging positions, the two water molecules, W728 and W729, are 3.8 Å from Phe M197 and His L168, respectively. The other three water molecules, W723, W736, and W737, are also close to the amino acid residues that were replaced to establish H-bonds with P. W723 is 5.5 Å from Leu L131 and 7.2 Å from the 9-keto carbonyl group of P_L. W736 is 4.3 Å from Phe M197 and 5.1 Å from ring B of P_M. W737 is 7.3 Å from His L168 and 4.1 Å from ring D of P_L. In each case, these water molecules are aligned with the Q_x or Q_y transition of P or one of the B monomers. Previous studies have led to the proposal that W728 when H-bonded to the 9-keto carbonyl of B_L facilitates the ultrafast charge separation (*44*). It was demonstrated that introducing a positively charged Arg at the L181 position causes the displacement of W729 by ~5 Å that allowed this water molecule to serve as the sixth ligand to the central Mg^{2+} of B_M (*45*). One might speculate that the introduction of a positively charged His residue placed at L131 or M197 or, correspondingly, the replacement of His L168 with Phe may cause similar displacements of W723, W728, and W729 in the mutants with these substitutions. In the crystal structure of the mutant containing all three mutations at L131, M160, and M197, changes in the location of the water molecules were not modeled because of the limited resolution of the diffraction data (*35*). As demonstrated in Figure 2, the formation or removal of H-bonds with protons donated by histidine shifts the positions of the Q_y bands of the dimer substantially. Similarly, the formation of the H-bonds increased the potential of the dimer in all cases (*36*). The putative H-bonds between the 9-keto carbonyls of B_A and B_B with W728 and W729 should also influence these bands and are probably altered by the replacement of Phe M197 and His L168, respectively. These observations are all consistent with the stabilization of the positive charge on P by dielectric relaxation upon illumination in WT and in those mutants where the conformational changes leading to the long-lived charge-separated states are favored. Because W737 and W736 are along the Q_x transitions of P_L and P_M, any movement would be expected to cause a shift in the Q_x band of the bacteriochlorophylls around 600 nm. The spectra recorded immediately after the onset of the illumination and 1 min after the 1 min illumination had ended showed a 15 nm blue shift of this band from 601 to 586 nm (data not shown). A detailed investigation of the blue shift in the Q_x bands in the mutants and the potential role of the W737 and W736 water molecules in the light-induced conformational changes is underway. Additional work is in progress to address the potential perturbation caused by detergent micelles. These studies investigate RCs that are dispersed in various detergents and in liposomes containing lipids with different headgroup charges and systematically altered hydrophobic chain lengths.

SUPPORTING INFORMATION AVAILABLE

Dependence of the position of the Q_y band of P, the position of the positive peak of the electrochromic absorption change of B molecules, and the spin density distribution on the number of H-bonds; light-induced electrochromic absorption changes in B_M and B_L deduced from near-infrared light-minus-dark absorption difference spectra for 11 mutants and the WT; and fitting parameters for the electrochromic absorption changes of B molecules. This material is available free of charge via the Internet at http://pubs.acs.org.

REFERENCES

1. Hunter, C. N., Daldal, F., Thurnauer, M. C., and Beatty, J. T., Eds. (2008) The Purple Phototropic Bacteria, Springer-Verlag, Dordrecht, The Netherlands.
2. Allen, J. P., Feher, G., Yeates, T. O., Komiya, H., and Rees, D. C. (1987) Structure of the reaction center from *Rhodobacter sphaeroides* R-26: The cofactors. *Proc. Natl. Acad. Sci. U.S.A. 84*, 5730–5734.
3. Allen, J. P., Feher, G., Yeates, T. O., Komiya, H., and Rees, D. C. (1987) Structure of the reaction center from *Rhodobacter sphaeroides* R-26: The protein subunits. *Proc. Natl. Acad. Sci. U.S.A. 84*, 6162–6166.
4. Steffen, M. A., Lao, K., and Boxer, S. G. (1994) Dielectric asymmetry in the photosynthetic reaction center. *Science 264*, 810–816.
5. Premvardhan, L. L., van der Horst, M. A., Hellingwerf, K. J., and van Grondelle, R. (2003) Stark spectroscopy on photoactive yellow protein, E46Q, and a nonisomerizing derivative, probes photo-induced charge motion. *Biophys. J. 84*, 3226–3229.
6. Mattioli, T. A., Lin, X., Allen, J. P., and Williams, J. C. (1995) Correlation between multiple hydrogen bonding and alteration of the oxidation potential of the bacteriochlorophyll dimer of *Rhodobacter sphaeroides*. *Biochemistry 34*, 6142–6152.
7. Peloquin, J. M., Williams, J. C., Lin, X., Alden, R. G., Taguchi, A. K. W., Allen, J. P., and Woodbury, N. W. (1994) Time dependent thermodynamics during early electron transfer in reaction centers from *Rhodobacter sphaeroides*. *Biochemistry 33*, 8089–8100.
8. Moser, C. C., Keske, J. M., Warncke, K., Farid, R. S., and Dutton, P. L. (1992) Nature of biological electron transfer. *Nature 355*, 796–802.
9. Malkin, S., Churio, M. S., Shochat, S., and Braslavsky, S. E. (1994) Photochemical energy storage and volume changes in the microsecond time range in bacterial photosynthesis: A laser induced optoacoustic study. *J. Photochem. Photobiol., B 23*, 79–85.
10. Mauzerall, D. C., Gunner, M. R., and Zhang, J. M. (1995) Volume contraction on photoexcitation of the reaction center from *Rhodobacter sphaeroides* R-26: Internal probe of dielectrics. *Biophys. J. 68*, 275–280.
11. Tiede, D. M., Vazquez, J., Cordova, J., and Marone, P. A. (1996) Time-resolved electrochromism associated with the formation of quinone anions in the *Rhodobacter sphaeroides* R26 reaction center. *Biochemistry 35*, 10763–10775.
12. Li, J., Gilroy, D., Tiede, D. M., and Gunner, M. R. (1998) Kinetic phases in the electron transfer from $P^+Q_A^-Q_B$ to $P^+Q_AQ_B^-$ and the associated processes in *Rhodobacter sphaeroides* R-26 reaction centers. *Biochemistry 37*, 2818–2829.
13. Graige, M. S., Feher, G., and Okamura, M. Y. (1998) Conformational gating of the electron transfer reaction $Q_A^{-\bullet}Q_B \rightarrow Q_AQ_B^{-\bullet}$ in bacterial reaction centers of *Rhodobacter sphaeroides* determined by a driving force assay. *Proc. Natl. Acad. Sci. U.S.A. 95*, 11679–11684.
14. Puchenkov, O. V., Kopf, Z., and Malkin, S. (1995) Photoacoustic diagnostics of laser-induced processes in reaction centers of *Rhodobacter sphaeroides*. *Biochim. Biophys. Acta 1231*, 197–212.
15. Goushcha, A. O., Kharkyanen, V. N., and Holzwarth, A. R. (1997) Nonlinear light-induced properties of photosynthetic reaction centers under low intensity irradiation. *J. Phys. Chem. B 101*, 259–265.
16. Kálmán, L., and Maróti, P. (1997) Conformation-activated protonation in reaction center of the photosynthetic bacterium *Rhodobacter sphaeroides*. *Biochemistry 36*, 15269–15276.
17. van Mourik, F., Reus, M., and Holzwarth, A. R. (2001) Long-lived charge separated states in bacterial reaction centers isolated from *Rhodobacter sphaeroides*. *Biochim. Biophys. Acta 1504*, 311–318.
18. Andréasson, U., and Andréasson, L. E. (2003) Characterization of a semi-stable charge-separated state in reaction centers from *Rhodobacter sphaeroides*. *Photosynth. Res. 75*, 223–233.
19. Wang, H., Lin, S., Allen, J. P., Williams, J. C., Blankert, S., Laser, C., and Woodbury, N. W. (2007) Protein dynamics control the kinetics of initial electron transfer in photosynthesis. *Science 316*, 747–750.
20. Olenchuk, M., and Berezetska, N. (2008) Study of the recombination process of light-induced charge separation in reaction centers of

purple bacteria under long-term exposition. *Mol. Cryst. Liq. Cryst. 497*, 121–128.
21. Stowell, M. H. B., McPhillips, T. M., Rees, D. C., Soltis, S. M., Abresch, E., and Feher, G. (1997) Light-induced structural changes in photosynthetic reaction center: Implications for mechanism of electron-proton transfer. *Science 276*, 812–816.
22. Katona, G., Snijder, A., Gourdon, P., Andréasson, U., Hansson, Ö., Andréasson, L. E., and Neutze, R. (2005) Conformational regulation of charge recombination reactions in a photosynthetic bacterial reaction center. *Nat. Struct. Mol. Biol. 12*, 630–631.
23. Chang, C. H., El-Kabbani, O., Tiede, D., Norris, J. R., and Schiffer, M. (1991) Structure of the membrane-bound protein photosynthetic reaction center from *Rhodobacter sphaeroides*. *Biochemistry 30*, 5352–5360.
24. Arnoux, B., Gaucher, J. F., Ducruix, A., and Reiss-Husson, F. (1995) Structure of the photochemical reaction center of spheroidine-containing purple bacterium *Rhodobacter sphaeroides* at 3 Å resolution. *Acta Crystallogr. D51*, 368–379.
25. Allen, J. P., and Williams, J. C. (1995) Relationship between the oxidation potential of the bacteriochlorophyll dimer and electron transfer in photosynthetic reaction centers. *J. Bioenerg. Biomembr. 27*, 275–281.
26. Mattioli, T. A., Williams, J. C., Allen, J. P., and Robert, B. (1994) Changing in primary donor hydrogen-bonding interactions in mutant reaction centers from *Rhodobacter sphaeroides*. Identification of all vibrational frequencies of all conjugated carbonyl groups. *Biochemistry 33*, 1636–1643.
27. Nabedryk, E., Allen, J. P., Taguchi, A. K. W., Williams, J. C., Woodbury, N. W., and Breton, J. (1993) Fourier-transform infrared study of the primary electron donor in chromatophores of *Rhodobacter sphaeroides* with reaction centers genetically modified at residue M160 and residue L131. *Biochemistry 32*, 13879–13885.
28. Rautter, J., Lendzian, F., Shulz, C., Fetsch, A., Kuhn, M., Lin, X., Williams, J. C., Allen, J. P., and Lubitz, W. (1995) ENDOR studies of the primary donor cation radical in mutant reaction centers of *Rhodobacter sphaeroides* with altered hydrogen-bond interactions. *Biochemistry 34*, 8130–8143.
29. Williams, J. C., Alden, R. G., Murchison, H. A., Peloquin, J. M., Woodbury, N. W., and Allen, J. P. (1992) Effects of mutations near the bacteriochlorophylls in reaction center from *Rhodobacter sphaeroides*. *Biochemistry 31*, 11029–11037.
30. Williams, J. C., Alden, R. G., Coryell, V. H., Lin, X., Murchison, H. A., Peloquin, J. M., Woodbury, N. W., and Allen, J. P. (1992) Changes in the oxidation potential of the bacteriochlorophyll dimer due to hydrogen bonds in reaction centers from *Rhodobacter sphaeroides*. Research in Photosynthesis, Vol. 1, pp 377−380, Kluwer Academic Publishers, Dordrecht, The Netherlands.
31. Murchison, H. A., Alden, R. G., Allen, J. P., Peloquin, J. M., Taguchi, A. K. W., Woodbury, N. W., and Williams, J. C. (1993) Mutations designed to modify the environment of the primary electron donor of the reaction center from *Rhodobacter sphaeroides* phenylalanine to leucine at L167 and histidine to phenylalanine at L168. *Biochemistry 32*, 3498–3505.
32. Paddock, M. L., Rogney, S. H., Feher, G., and Okamura, M. Y. (1989) Pathway of proton transfer in bacterial reaction centers: Replacement of glutamic acid 212 in the L-subunit with glutamine inhibits the quinone (secondary acceptor) turnover. *Proc. Natl. Acad. Sci. U.S.A. 86*, 6602–6606.
33. Parson, W. W. (2007) Electronic absorption. In Modern Optical Spectroscopy, pp 182−188, Springer-Verlag, Berlin.
34. Kálmán, L., LoBrutto, R., Narváez, A. J., Williams, J. C., and Allen, J. P. (2003) Correlation of proton release and electrochromic shifts of the optical spectrum due to oxidation of tyrosine in reaction centers from *Rhodobacter sphaeroides*. *Biochemistry 42*, 13280–13286.
35. Thielges, M., Uyeda, G., Cámara-Artigas, A., Kálmán, L., Williams, J. C., and Allen, J. P. (2005) Design of a redox-linked active metal site: Manganese bound to bacterial reaction centers at a site resembling that of photosystem II. *Biochemistry 44*, 7389–7394.
36. Lin, X., Murchison, H. A., Nagarajan, V., Parson, W. W., Allen, J. P., and Williams, J. C. (1994) Specific alteration of the oxidation potential of the electron donor in reaction centers from *Rhodobacter sphaeroides*. *Proc. Natl. Acad. Sci. U.S.A. 91*, 10265–10269.
37. Kleinfeld, D., Okamura, M. Y., and Feher, G. (1984) Electron transfer in reaction centers of *Rhodopseudomonas sphaeroides*. I. Determination of the charge recombination pathway of $D^+Q_AQ^-_B$ and free energy and kinetic relations between $Q^-_AQ_B$ and $Q_AQ^-_B$. *Biochim. Biophys. Acta 766*, 126–140.
38. Kleinfeld, D., Okamura, M. Y., and Feher, G. (1984) Electron-transfer kinetics in photosynthetic reaction centers cooled to cryogenic temperatures in the charge-separated state: Evidence for light-induced structural changes. *Biochemistry 23*, 5780–5786.
39. Xu, Q., and Gunner, M. R. (2001) Trapping conformational intermediate states in the reaction center protein from photosynthetic bacteria. *Biochemistry 40*, 3232–3241.
40. Fritzsch, G., Koepke, J., Diem, R., Kuglstatter, A., and Baciou, L. (2002) Charge separation induces conformational changes in the photosynthetic reaction centre of purple bacteria. *Acta Crystallogr. D58*, 1660–1663.
41. Breton, J. (2004) Absence of large-scale displacement of quinone Q_B in bacterial photosynthetic reaction centers. *Biochemistry 43*, 3318–3326.
42. Breton, J. (2007) Steady-state FTIR spectra of the photoreduction of Q_A and Q_B in *Rhodobacter sphaeroides* reaction centers provide evidence against the presence of a proposed transient electron acceptor X between the two quinones. *Biochemistry 46*, 4459–4465.
43. Ermler, U., Fritzsch, G., Buchanan, S. K., and Michel, H. (1994) Structure of the photosynthetic reaction center from *Rhodobacter sphaeroides* at 2.65 Å resolution. Cofactors and protein-cofactor interactions. *Structure 2*, 925–936.
44. Potter, J. A., Fyfe, P. K., Frolov, D., Wakeham, M. C., van Grondelle, R., Robert, B., and Jones, M. R. (2005) Strong effects of an individual water molecule on the rate of light-driven charge separation in the *Rhodobacter sphaeroides* reaction center. *J. Biol. Chem. 280*, 27155–27164.
45. Frolov, D., Marsh, M., Crouch, L. I., Fyfe, P. K., Robert, B., van Grondelle, R., Hadfield, A., and Jones, M. R. (2010) Structural and spectroscopic consequences of hexacoordination of a bacteriochlorophyll cofactor in the *Rhodobacter sphaeroides* reaction center. *Biochemistry 49*, 1882–1892.